Iranian Journal of Fisheries Sciences 21(4) 864-879 2022
DOI: 10.22092/ijfs.2022.127361

Research Article

Otolith shape utilization for the stock identification of Caroun croaker, *Johnius carouna* (Cuvier, 1830) (Perciformes: Sciaenidae), from the east Vietnam sea

Vu Q.T. [1*]; Tran V.D. [1]; Nguyen V.Q.[2]

Received: May 2022 Accepted: June 2022

Abstract

Based on the climate hydrology, ecological biogeography, and land–sea interaction relationships, Vietnamese coastal waters can be separated into three coastal zones. In this study, we analyzed the *Johnius carouna* (Cuvier, 1830) shape of sagittae from several areas along the Vietnamese coast. The morphometric characters of the otoliths were used to identify stock among the fish of different geographic areas. A multistatistics analysis of otolith shapes was applied to estimate the differences between the three regions. Based on the shape indices, wavelet transform and Elliptic Fourier Descriptors (EFD) have signals for division into three groups of otolith shapes (discriminant analysis for wavelet transform: Wilks=0.065, $p<0.001$ training misclassification error 9.8%; discriminant analysis EFD: Wilks=0.059, $p<0.001$ accuracies of the classification equal 93.75%; analysis of variance on shape indices: $p<0.05$) of the otoliths for the three locations. This study inferred that two distinct stocks were identified, namely Cat Ba and Tho Chu. The individuals from the central zone (Phu Yen) may be a mixing zone between the north and the south, with two possible populations of Cat Ba and Tho Chu.

Keywords: *Johnius carouna*, Caroun croaker, Discriminant analysis, Wavelet transform, East Vietnam Sea.

1-Vietnam-Russia Tropical Center; Nguyen Van Huyen, Hanoi, Vietnam
2- Vietnam Academy of Science and Technology, Hanoi, Vietnam
*Corresponding author's Email: vuquyetthanh@gmail.com

Introduction

Otoliths are calcium carbonate structures (otoliths and ear stones) of bony fishes (except lampreys), which aid in balancing and hearing. There are three pairs of otoliths in each fish, including two small pairs (lapilli and asteriscii) and one large pair (the sagittae) Schulz-Mirbach *et al*., 2014; Santos *et al*., 2017). Studies have been shown that the sagittal otolith shape is also related to swimming (Volpedo and Echeverra, 2003) and stock distribution (Lombarte and Cruz, 2007; Sadighzadeh *et al*., 2014; Tuset *et al*., 2016). The morphometric characteristics of otoliths have been widely used to differentiate species for identifying stocks (Stransky *et al*., 2008; Tuset *et al*., 2012; Bani *et al*., 2013). Furthermore, the records of growth and development of individual fishes are retained in otoliths (Campana and Neilson, 1985; Hosseini-Shekarabi *et al*., 2014; Yedier, 2021). Several studies have widely used sagittal otolith shapes to identify species, populations, and stocks (Osman *et al*., 2020; Ghanbarifardi and Zarei, 2021). In numerous cases, variations in sagittal shape can be associated with the biological uniqueness of species and fish stocks (Campana and Casselman, 1993; Stransky, 2005; Vu and Kartavsev, 2020). A recent study used otolith morphology as a tool to identify stocks of the species *Hypomesus japonicus*. Their findings suggest the existence of at least two local stocks of the species in the waters of the North-western Sea of Japan (Vu and Kartavsev, 2020). The analysis of otolith shape was used to determine the stock structure of European anchovy (*Engraulis encrasicolus*) along the Tunisian coast. The results of the study identified the existence of three distinct stock units of *E. encrasicolus*. These findings will have major implications for fisheries management (Khemiri *et al.*, 2018).

Elliptical Fourier Descriptors (EFDs), wavelet transform (WT), and shape index (ShI; circularity, roundness, rectangularity, form factor, aspect ratio, and ellipticity) are the standard methods used for the analysis of otolith shapes (Burke *et al*., 2009, Keating and Brophy, 2014; Mapp *et al*., 2017). The results of these analyses are used to delineate fish stocks (Agüera and Brophy, 2011; Paul *et al*., 2013; Ferhani *et al*., 2021).

EFDs analysis can be used for the description of a closed contour. A closed contour is a periodic function of a parameter and can be represented as a total of sine and cosine functions of growing frequencies, which are affected by coefficients called normalized elliptic Fourier (NEF). The total of these sine and cosine functions converges toward the initial border as the number of harmonics increases. Each harmonic is an ellipse, which is completely defined by its period and NEF (Campana and Casselman 1993, Godefroy *et al*., 2012). In otolith two-dimensional (2D) image analysis, WT is used to describe otolith shape using wavelet descriptors. Further, it is used to recognize otoliths according to their contour shape by obtaining wavelet coefficients. WT uses functions in finite domains, making them well-

suited for sharp edges (Libungan and Pálsson, 2015).

Globally, croakers or drums are important fishery resources in shallow warm seas and estuaries. Caroun croaker is a commercial fish extensively distributed in the tropical and temperate seas along the western coasts of the Indo-West Pacific. A study in Thailand suggested that croakers are important economic species commonly found during coastal fishing. The current fishing pressure is slightly high; the mature size of Caroun croakers is 15.3 cm, and the average catch size is 15.12 cm, which is smaller than the mature size (Sawusdee and Rattanarat, 2021). The maximum standard length of this fish is 25 cm, and the average standard length is 16 cm (Froese and Pauly, 2022).

Based on climate hydrology, ecological biogeography, and land–sea interactions, the Vietnamese coastal region can be divided into three coastal zones. Caroun croaker (*J. carouna*) specimens were collected from several fishing points in Cat Ba (CB; North zone), Phu Yen (PY; transitional zone), and Tho Chu (TC; South zone). This study aimed to describe the morphometric characteristics of sagittal otoliths and provide information regarding the stock structure of this species in three fishery regions (CB, PY, and TC) in the East Sea of Vietnam using three otolith shape approaches (WT, EFD, and ShI).

Materials and methods

Fish Sampling

Individuals were captured by trawling from three regions in the East Sea of Vietnam. Caroun croakers with a total length of 16–19 cm were sampled. In this study, 176 left otoliths were collected: 49 from CB, 50 from PY, and 77 from TC. All otoliths were extracted from fishes collected from fish landing sites (Fig. 1).

Image acquisition, digitization, and shape index

Each otolith was placed against a black background and was standardized by positioning them with the rostrum oriented to the left (Fig. 2). The left sagittae was photographed using an Olympus SZ61 zoom stereo microscope. Digital images of otoliths were captured under a stereomicroscope using Olympus CellSens (version 2.2) with an SC180 camera and saved in JPG and BMP formats. The characteristics of otoliths were measured (in mm) and analyzed based on ShIs. To determine the morphometric characteristics of otoliths, four basic dimensional parameters, namely area (A), perimeter (P), otolith width (OW), and otolith length (OL), were automatically measured using the ShapeR package in R (Libungan and Pálsson, 2015).

Six common ShIs were calculated using the ratios of OW, OL, A, and P (Agüera and Brophy 2011) as follows: aspect ratio=OL/OW; ellipticity= (OL−lOW)/ (OL+OW); circularity=P^2/A; rectangularity=A/

(OL×OW); roundness=4A/OL^2; and form factor=4 × A/P^2 (Agüera and Brophy, 2011; He *et al*., 2017).

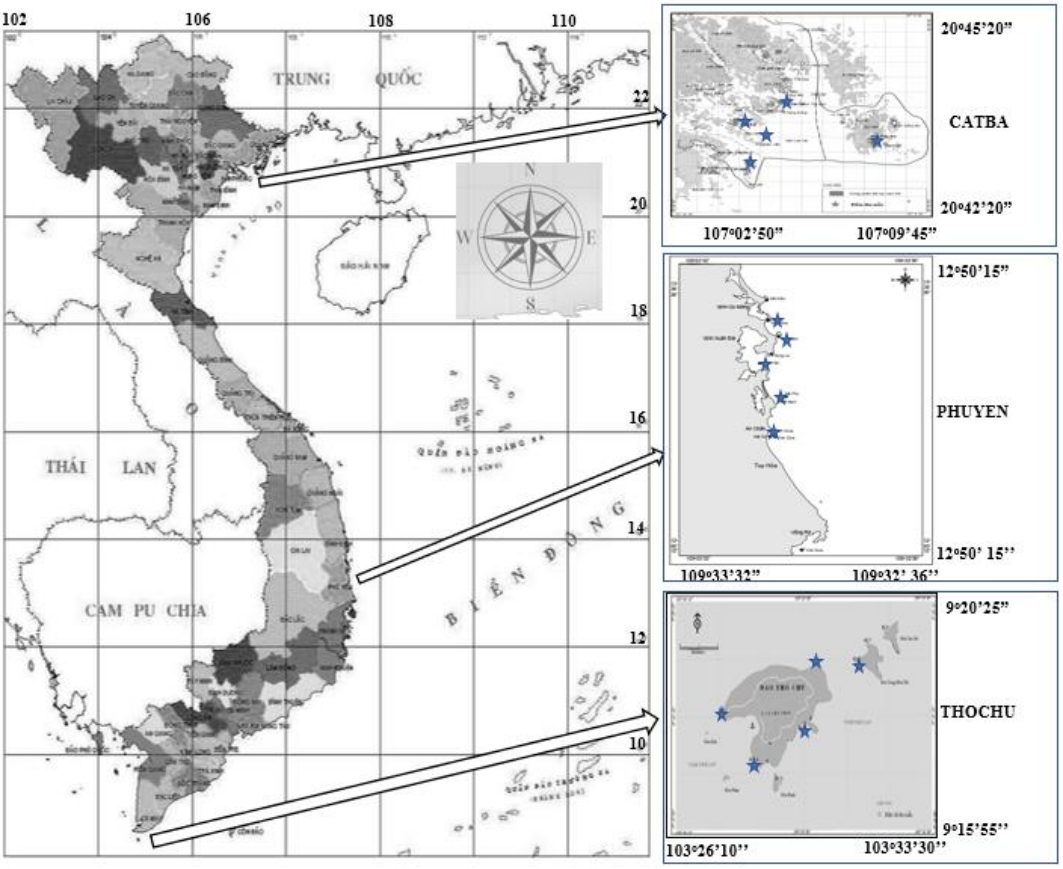

Figure 1: Sampling locations of J. carouna along the Vietnamese coast. ***The blue stars indicate specific fishing points.***

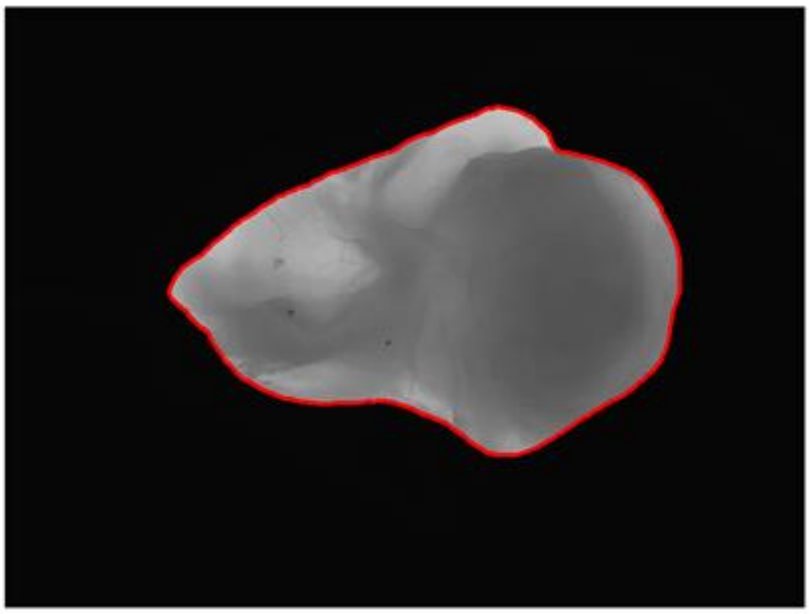

Figure 2: Sagittae otolith of *J. carouna.*

EFDs can be used to outline shapes with a closed 2D contour (Kuhl and Giardina, 1982). EFD analysis was performed using two methods: Shape version 1.3 for extracting EFDs with 20 harmonics and the ShapeR package for extracting EFDs with 2 harmonics.EFDs (20 harmonics) for contouring reconstruction. Using Shape version 1.3, EFD was extracted from the JPG image with 20 harmonics, as described in a study by Iwata and Ukai (2002). Shape version 1.3 was used to standardize size and orientation, providing the first three fixed coefficient values of a_1=1 and b_1=c_1=0. Each harmonic comprised four coefficients, resulting in 80 (4×20 harmonics) coefficients per otolith. Therefore, each individual was represented by 77 (80−3) unique coefficients (He *et al*., 2017). These 77 coefficients were used to contour reconstruction using PrintComp and PrintPrint (subprograms of Shape version 1.3).

Using the R software, the Shape-R package extracted EFDs with 12 harmonics from the BMP image according to the instructions of a previous study. This was performed to generate 12 harmonics for each sample. Each harmonic was composed of four NEFs and yielded 12×4=48 NEFs. The first three coefficients were omitted due to the standardization with respect to size, providing the first three fixed coefficient values of a_1=1 and b_1=c_1=0. Thus, this analysis initially used 48−3=45 NEFs per individual. Canonical analysis of principal coordinates (CAP) and discriminant analysis were performed using EFD (12 harmonics). The ShapeR package was used to extract wavelet coefficients of the otolith outline for wavelet shape analysis. Each sagittae was represented by 64 wavelet coefficients (Libungan and Pálsson, 2015). WTs were used to outline delineation in statistical analysis.

Data analysis

For all input data, normality was ensured by Kolmogorov–Smirnov test in R (*p*-value>0.05), and, when necessary, data were $\log_{10}$-transformed. Using the vegan, ggplot, and haper packages in R, canonical analysis of principal coordinates (CAP) was performed using WT and EFD (12 harmonics) to compare otolith shape variations among the sample populations (Anderson and Willis, 2003; Libungan and Pálsson, 2015). The successful classification of the discriminant analysis was assessed by cross-validation (MASS and ipred packages in R). The significant principal components (PCs) were established according to the method described by Duarte - Neto *et al*. (2008). Using the FactoMineR and factoextra packages, the PC scores in the multivariate analysis were used to determine ShIs, and the rpart package was used to calculate the multiclass response for ShIs (Therneau and Atkinson, 2017).

Results

Image and outline delineation of J. carouna

Outline delineation based on WT, ShI, PPC and EFD

The analysis of reconstructed otolith contours revealed differences among the three locations. The patterns in Figure 3 a and b clearly show that most group variations can be found in the following three angle ranges of the otolith: 50°–70°, 170°–180°, and 260°–300°.

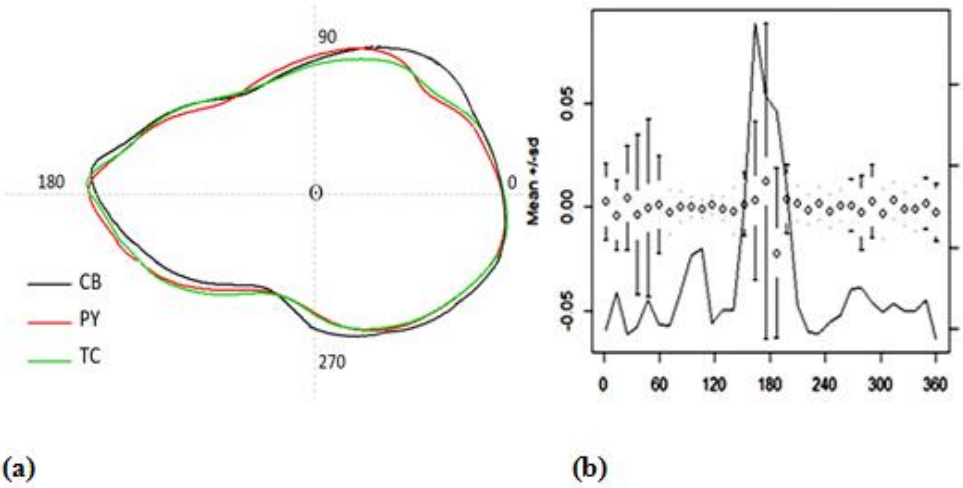

Figure 3: (a) Average sagittal shape based on wavelet transform (WT) rebuilding for *(J. carouna*) from the East Sea of Vietnam. The numbers (0°, 90°, 180°, and 270°) are angles in polar coordinates. The symbol ⊙ indicates the centroid of the sagittal and the center point of the polar coordinates. The average sagittal otolith shapes show distinct differences among the three sites. (b) Average and squared deviation (sd) of WT for combined sagittal otoliths and the proportion of variance among the three areas. The horizontal axis shows the angle based on polar coordinates, where the centroid of the otolith is the center point of the polar coordinates.

Contour reconstruction based on EFD (20 harmonics) for *J. carouna* from the East Sea of Vietnam revealed three sagittal morphotypes. Individuals from PY showed mixed morphotypes from the other two regions (Fig. 4).

ShI was examined using one-way analysis of variance (ANOVA) to detect the differences among the three locations (F-test>1, $p<0.05$). Several comparisons showed that the overall otolith shape contours and ShI significantly differed among the three regions (CB, TC, and PY), indicating that the sagittal shapes of individuals from CB and TC were unique as there was no overlap in shape traits between them. The sagittae of *J. carouna* specimens from CB significantly differed from those of TC in circularity, rectangularity, roundness, ellipticity, and aspect ratio (Table 1).

A model with a multiclass response for ShI at three sites also showed close similarities between individuals from PY and TC areas in aspect ratio (node: 1.3<aspect ratio<1.5) and between individuals from CB and TC areas in aspect ratio (node: 1.3) (Fig. 5).

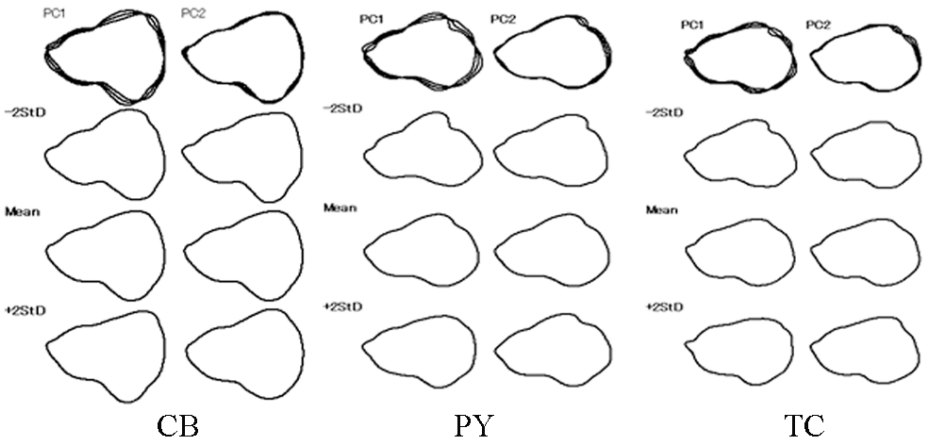

Figure 4: The sagittal shape means of EFD (20 harmonics) and ranges for the first two principal components. Note: Means indicate reconstruction mean; ± 2SD: ± standard deviation; CB: Cat Ba; PY: Phu Yen; TC: Tho Chu.

Table 1: Comparison of otolith shape indices (ShIs) among three locations using averages and analysis of variance.

Sites/F, p	Average ± SE, CB	Average ± SE, PY	Average ± SE, TC	F-test of ANOVA	*p*
Circularity	15.10 ± 0.04	15.13 ± 0.11	15.11 ± 0.08	0.153	0.85 > 0.05
Rectangularity	0.650 ± 0.001	0.671 ± 0.001	0.696 ± 0.001	92.3	0.001 < 0.05
Form factor	0.83 ± 0.001	0.82 ± 0.001	0.84 ± 0.001	0.11	0.013 < 0.05
Roundness	0.221 ± 0.001	0.195 ± 0.01	0.181 ± 0.001	100.1	0.001 < 0.05
Ellipticity	0.091 ± 0.001	0.186 ± 0.001	0.191 ± 0.001	117.1	0.001 < 0.05
Aspect ratio	1.100 ± 0.002	1.411 ± 0.013	1.575 ± 0.005	15.9	0.0024 < 0.05

Note: SE, standard error; CB: Cat Ba; PY: Phu Yen; TC: Tho Chu

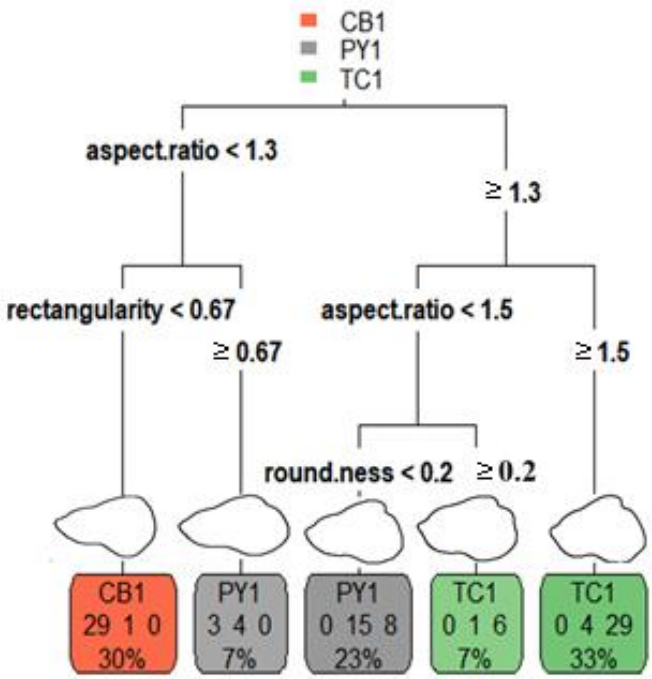

Figure 5: A model with a multiclass response for ShI at three sites. Each node displays the predicted class, predicted probability, and percentage of observations in the node. Predicted classes: CB, PY, and TC; predicted probability of each class. Note: CB: Cat Ba; PY: Phu Yen; and TC: Tho Chu.

Scatterplots of the first two axes (PC–PC1 and PC–PC2; Fig. 6) were used to differentiate the three morphotypes (Fig. 3a, b). Comparative analysis of PCs indicated that the first two PCs were occupied, accounting for 93.2% of the overall variance. PC1, which accounted for 60.7% of the total variance, was mainly determined using four ShIs (rectangularity, roundness, form factor ellipticity, and aspect ratio). PC2, which accounted for 32.5% of the total variance, was mainly determined using circularity and form factors. Figure 6 shows the overlapped distribution of the PY and TC areas of the Caroun croaker. CB specimens were primarily distributed in the second and third quadrants, whereas TC and PY specimens were mainly observed in the first and fourth quadrants.

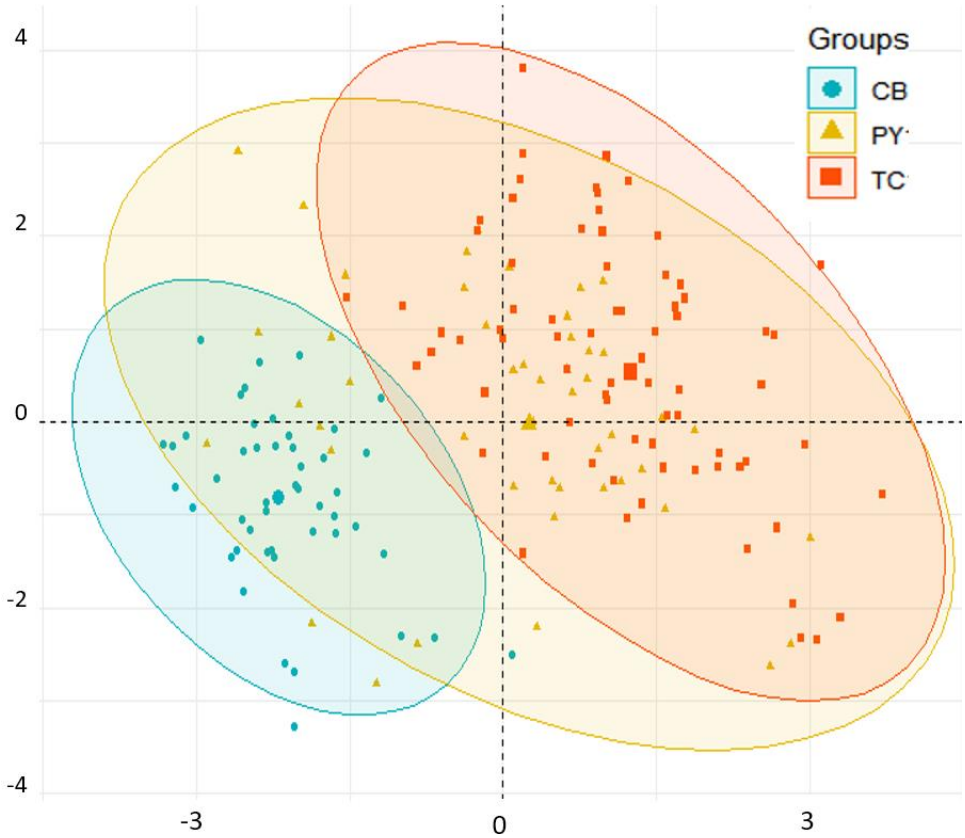

Figure 6: Distribution of the individual ordination plots of the first two principal components (PC1 and PC2) in the left otolith shape analysis using ShI at the three sites. The first two PCs accounted for 60.7% and 32.5% of the total variance in otolith shape.

In CAP, the canonical correlation of CAP1 was 92.9% and that of CAP2 was 7.1%, indicating a difference between otolith shapes in the three regions (CB, PY, and TC). The scatterplot of CAP1 and CAP2 separated the two distinct regions: CB and TC (Fig. 7). Individuals from TC and PY overlapped and were primarily distributed in the positive part of the horizontal axis, whereas those from CB were mainly observed in the negative part of the horizontal axis (CAP1).

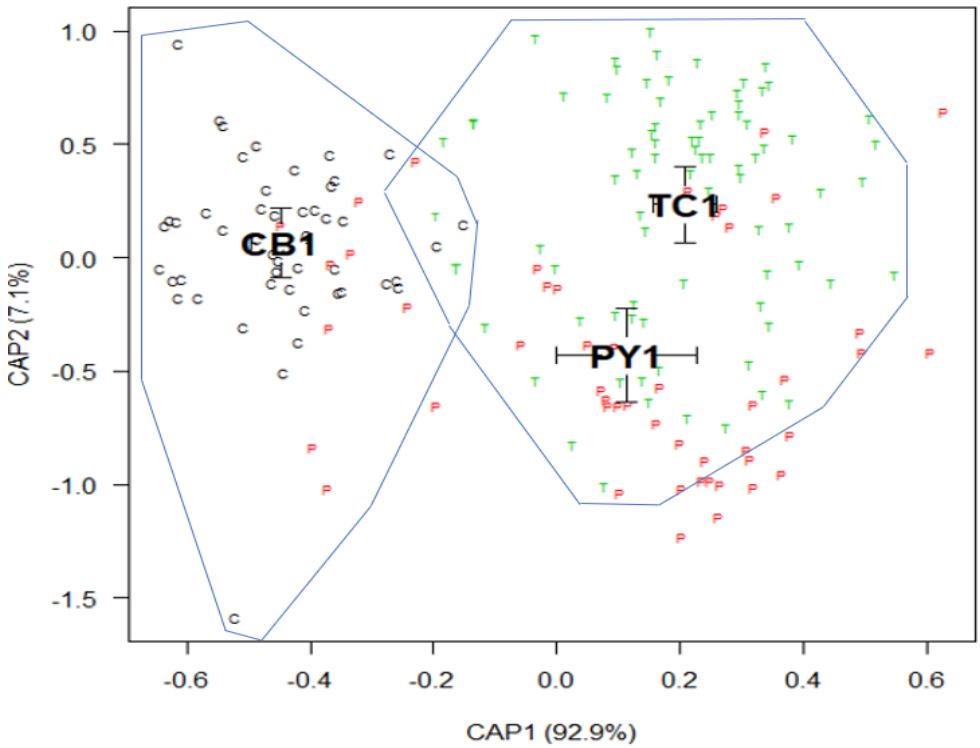

Figure 7: Scatterplot of CAP1 and CAP2 with EFD (12 harmonics) from the analysis of *J.carouna* otoliths obtained from three regions. Black characters represent the mean canonical value for each region. Canonical scores on the first two discriminating axes, CAP1 and CAP2, are shown. Note: CB: Cat Ba; PY: Phu Yen; and TC: Tho Chu.

Training EFD (12 harmonics) misclassification

The training misclassification error in the discriminant analysis (Wilks=0.059, F=11.93, p<0.001) was 6.25%, and the mean accuracy of the classification was 93.75% in otoliths for the three regions (CB, TC, and PY). The classification matrix provided more information regarding accurately identifying individuals from TC as 94% and CB as 97%. Overall, 5 of the 77 specimens were low misclassified between PY and TC (equivalent to 6%), whereas 1 of 49 specimens were low misclassified between PY and CB (equivalent to 3%; Table 2). There was no classification error between the CB and TC specimens.

Table 2: Matrix of classification using linear discriminant analysis based on elliptic Fourier descriptors (with 12 harmonics).

Classified group	CB, p<0.001	PY, p<0.001	TC, p<0.001	Classification accuracy %
CB	**48 (97%)**	1 (3%)	0	97
PY	2 (4%)	**44 (88%)**	4 (8%)	88
TC	0	5 (6%)	**72 (94%)**	94

Note: CB: Cat Ba; PY: Phu Yen; and TC: Tho Chu

For the wavelet coefficient analyses of 176 otoliths, the first discriminating axis (CAP1) accounted for 85.3% of the total variance among the three regions, namely CB, PY, and TC, whereas the second axis (CAP2) accounted for

14.7% (p<0.001). The harmonic coefficients were normalized by the first harmonic, and the shape analysis of the wavelet coefficients revealed significant differences among the average shapes of otoliths in the study area, CB, PY, and TC. The scatterplot of CAP1 and CAP2 separated the two distinct regions, CB and TC. There was an overlapping distribution of the characters of TC and PY in the CAP1 and CAP2 scatterplot (Fig. 8). The CB specimens were mainly distributed in negative CAP1, whereas TC was primarily located in the positive area. Individuals from TC and PY had the most similar wavelet coefficients, whereas those from CB and TC showed the most distinct wavelet coefficients in otolith shape across all locations.

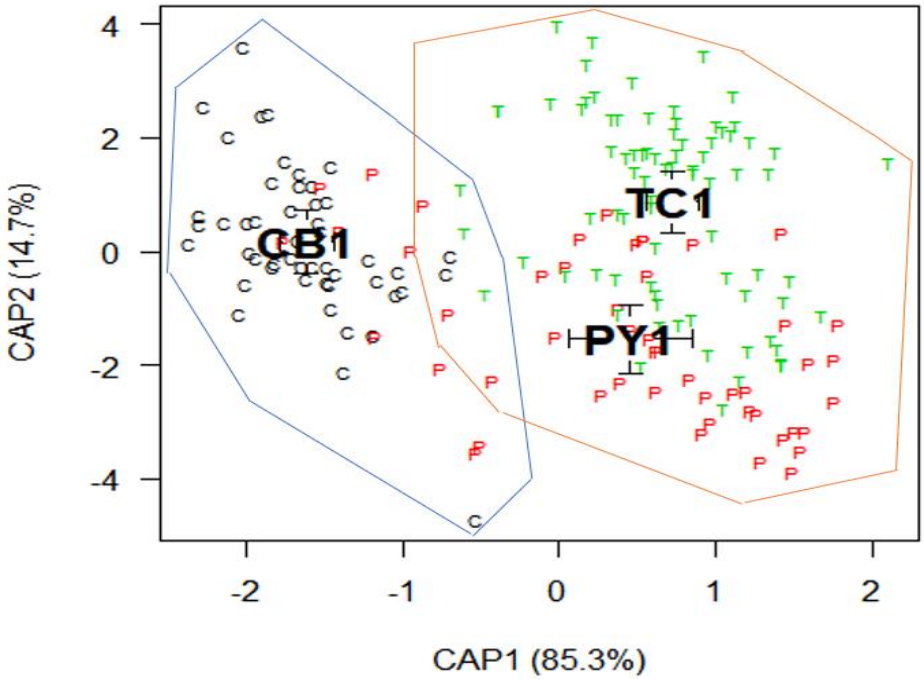

Figure 8: Sagittal otolith shape of specimens from three locations of *J. carouna* in the East Sea of Vietnam using CAP with WT. Black characters represent the mean canonical value for each location. Canonical scores on the first two discriminating axes, CAP1 and CAP2, are shown. Note: CB: Cat Ba; PY: Phu Yen; and TC: Tho Chu

Discriminant analysis was used for wavelet coefficient analysis to examine whether significant differences exist among the groups in terms of predictor variables and evaluate misclassification errors or percent correct classification. A training misclassification error of 9.8% (Wilks=0.065, F=6.85, p<0.001) indicated that 90.2% of the otoliths were correctly classified for the three regions (CB, TC, and PY). Linear discriminant analysis was used to further support the separation of the three regions under study, with variability among otolith shapes inferring three stocks of CB–PY–TC. The linear discriminant analysis results based on wavelet coefficients of the sagittae revealed a PY–CB misclassification of 6% and a PY–TC misclassification of 12% (Table 3). No classification error was observed between the CB and TC specimens. The

classification matrix in Table 3 shows that the classification accuracy of individuals from CB (95%) and TC (94%) was high, whereas that of individuals from PY was low (82%). The classification matrix and CAP results suggested that the stock in PY is probably a mixed population (Table 3).

Table 3: Matrix of classification using linear discriminant analysis based on Wavelet transforms (WT).

Classified group	CB, $p<0.001$	PY, $p<0.001$	TC, $p<0.001$	Classification accuracy %
CB	**47 (95%)**	2 (5%)	0 (0%)	95%
PY	3 (6%)	**41 (82%)**	6 (12%)	82%
TC	0 (0%)	5 (6%)	**72 (94%)**	94%

Note: CB: CatBa; PY: PhuYen; and TC: ThoChu

Discussion

Morphological analysis of sagittae is a widely applied tool in phylogenetic and population identification studies of fish species (Pavlov, 2019). Using a variation of sagittal morphology to discriminate populations, it is crucial to consider the factors that can alter the sagittal shape. The sagittal shape is a characteristic that reflects a combined effect of genetic and habitat factors, such as climate hydrology, ecology, and biogeography (Swain *et al*., 2005). Several studies on population identification have evaluated the relative importance of environmental conditions on sagittal shape (Burke *et al*., 2009). Many studies have been shown that numerous factors are responsible for population separation among the species, with the crucial elements being habitat and environmental conditions (Campana and Neilson, 1985; Cardinale *et al*., 2004; He *et al*., 2017).

Caroun croaker is a species known to be sensitive to environmental conditions. Based on climate hydrology, ecological biogeography, and land–sea interactions, the Vietnamese coastal region was divided into three coastal zones. The North zone (first zone), which ranges from Mong Cai (21°29′08.1″N, 108°03′50.4″E) to Hai Van cap (16°11′22.6″N, 108°07′46.6″E), is a part of Northern Vietnam and has a tropical monsoon sea and cold winter (in this study, CB is a representative of this zone). The transitional zone (second zone), ranging from Hai Van to Dai Lanh (12°50′08.0″N, 109°22′07.0″E), is a zone of interaction between the sea of southern Vietnam, which has a subequatorial monsoon, and the marine part of the North zone in the East Sea, which has a tropical monsoon. From the Dai Lanh cap to TC, the south zone is a sea characterized by a subequatorial monsoon sea and year-round warmth (Tran, 2015). For Caroun croakers, the total size range was between 16 and 18 cm, ensuring that all sampled examples were included, knowing that the length at first maturity was ~15.3 cm (Sawusdee and Rattanarat, 2021). The noise signal effect of growth and sexual

effect on sagittal otolith shape (Cardinale *et al*., 2004), which can alter the line contour of otoliths, were eliminated (Campana and Casselman, 1993). Delineation of the sagittal outline of *J. carouna* from three sites revealed the existence of three otolith morphologies corresponding to the three regions (Fig. 3a and b). However, the otolith morphologies of individuals from PY and TC did not differ greatly. In contrast, there was a clear difference between individuals from CB and TC. Different analytical methods based on ShI, WT, and EFD revealed that the division between the two regions, CB and TC, is entirely different.

CAP is a powerful tool of constrained ordination for ecology. It can perform a constrained ordination based on any distance. Ten wavelet levels yielded 64 wavelet constants using the Daubechies's least symmetry wavelet method (Hussy *et al*., 2016). CAP was used to import 64 wavelet coefficients into the canonical scope using interpoint dissimilarity to distribute monitoring and capture misclassification (Anderson and Willis, 2003). In CAP (with EFD and WT) plot, individuals from PY were scattered across the CB and TC space. The classification matrix results were similar, indicating that the classification accuracy between CB and TC individuals is 100% and between TC and PY is 94% (with WT) and 96% (with EFD, 12 harmonics), respectively. Caroun croakers from CB belonged to the north zone with the tropical monsoon sea and 4 months of cold winter with an average temperature of 16°C. In contrast, TC was characterized by a subequatorial monsoon sea and year-round warmth with an average temperature in winter of 26°C.In the present study, multiple comparisons have shown that the overall shape indices of *J. carouna* are very different between the three regions. The findings of this study are entirely in line with those found in previously published studies, as such as otolith shape analysis has been used to perform the identification of two smelt species specimens *Hypomesus japonicus* and *H. nipponensis* from the northwestern Sea of Japan (Vu and Kartavsev, 2020). The otolith analysis clearly supports the taxonomic distinctiveness of the species from body morphological comparison.

In conclusion, statistical analysis for otolith shapes could be used as a complementary approach to body morphological for distinguishing *J. carouna* species. Our results demonstrate the Caroun croaker stocks that were found in the East Vietnam Sea were divided into two distinct zones. Consequently, our findings will contribute to formulate a fisheries management strategy for *J. carouna*. In the future, we propose to study the genes of this species to clarify the differences between stocks and whether the phylogenetic origin is from North, Central or South.

Acknowledgments

This work was funded by the grant grants-in aids-aid from the Vietnam-Russia Tropical Center "Project Ecolan E 3.1, nhanh -17,18 UBPH" and partially

funded by the Grant a grant-in Aid-aid from the Vietnam Academy of Science and Technology (NVCC 23.02/22-23).

References

Agüera, A. and Deirdre, B., 2011. Use of sagittal otolith shape analysis to discriminate Northeast Atlantic and Western Mediterranean stocks of Atlantic saury, *Scomberesox saurus saurus* (Walbaum). *Fisheries Research*, 110, 465-471. http://dx.doi.org/10.1016/j.fishres.2011.06.003

Anderson, M.J. and Willis, T.J., 2003. Canonical analysis of principal coordinates: a useful method of constrained ordination for ecology. *Ecology*, 84, 511-525. https://doi.org/10.1890/0012-9658 (2003)084[0511: CAOPCA] 2.0.CO; 2

Bani, A., Poursaeid, S. and Tuset, V.M., 2013. Comparative morphology of the sagittal otolith in three species of south Caspian gobies. *Journal of Fish Biology*, 82, 1321-1332. https://doi.org/10.1111/jfb.12073

Burke, N., Brophy, D., Schön, P.J. and King, P.A., 2009. Temporal trends in stock origin and abundance of juvenile herring (*Clupea harengus*) in the Irish Sea. *ICES Journal of Marine Science, J. Conseil.*, 66(**8**),1749-1753. https://doi.org/10.1093/icesjms/fsp140

Campana, S. and Casselman, J., 1993. Stock Discrimination Using Otolith Shape-Analysis. *Canadian Journal of Fisheries and Aquatic Sciences*, 50(**5**), 1062-1083. http://dx.doi.org/10.1139/f93-123.

Campana, S.E. and Neilson, J.D., 1985. Microstructure of fish otoliths. *Canadian Journal of Fisheries and Aquatic Sciences*, 42, 1014-1032. https://doi.org/10.1139/f85-127

Cardinale, M., Doering-Arjes, M. and Mosegaard, H., 2004. Effects of sex, stock, and environment on the shape of known-age Atlantic cod (*Gadus morhua)* otoliths. *Canadian Journal of Fisheries and Aquatic Sciences*, 61, 158-167. https://doi.org/10.1139/f03-151.

CellSen, V., 2.2, https://www.olympus-lifescience.com/en/software/cellsens/, Accessed September 20, 2021.

Duarte-Neto, P., Lessa, R. and Stosic, B., 2008. The use of sagittal otoliths indiscriminating stocks of common dolphin fish (*Coryphaena hippurus*) off northeastern Brazil using multishape descriptors. *ICES Journal of Marine Science*, 7, 1144-1152. https://doi.org/10.1093/icesjms/fsn090

Ferhani, K., Bekrattou, D. and Mouffok, S., 2021. Inter-population morphological variability of the round sardinella (*Sardinella aurita* Valenciennes, 1847) in the Algerian Coast based on body morphometric, meristic and otolith shape. *Iranian Journal of Fisheries Sciences*, 20(**6**), 1757-1774. DOI: 10.22092/IJFS.2021.125491

Froese, R. and Pauly, D., 2022. FishBase, World Wide Web electronic publication,

www.fishbase.org, Accessed 18 march 2022).

Ghanbarifardi, M. and Zarei, R., 2021. Otolith shape analysis of three mudskipper species of Persian Gulf. *Iranian Journal of Fisheries Sciences*, 20(**2**), 333-342.

Godefroy, J.E., Bornert, F., Gros, I.C. and Constantinesco, A., 2012. Elliptical Fourier descriptors for contours in three dimensions: A new tool for morphometrical analysis in biology. *Comptes Rendus Biologies*, 335, 205-213. https://doi.org/10.1016/j.crvi.2011.12.004

He, T., Cheng, J., Qin, JG., Li,Y. and Gao, TX., 2017. Comparative analysis of otolith morphology in three species of Scomber. *Ichthyological Research*, 65, 192-201. http://doi.org/10.1007/s10228-017-0605-4

Hosseini-Shekarabi, S.P., Valinassab, T., Bystydzieńska, Z. and Linkowski, T., 2014. Age and growth of *Benthosema pterotum* (Alcock, 1890) (Myctophidae) in the Oman Sea. *Journal of Applied Ichthyology*, 31, 51-56. https://doi.org/10.1111/jai.12620

Hüssy, K., Mosegaar, H. and Albertsen, C.M., 2016. Evaluation of otolith shape as a tool for stock discrimination in marine fishes using Baltic Sea cod as a case study. *Fisheries Research*, 174, 210-218. http://dx.doi.org/10.1016/j.fishres.2015.10.010

Iwata, H. and Ukai, Y., 2002. SHAPE: A computer program package for quantitative evaluation of biological shapes based on elliptic Fourier descriptors. *Journal of Heredity*, 93, 384-385. https://doi.org/10.1093/jhered/93.5.384.

Keating, J.P. and Brophy, D., 2014. Officer, R.A., et al., Otolith shape analysis of blue whiting suggests a complex stock structure at their spawning grounds in the Northeast Atlantic. *Fisheries Research*, 157, 1-6. https://doi.org/10.1016/j.fishres.2014.03.009

Khemiri, S., Gaamour A., Abdallah, L.B. and Fezzani S., 2018. The use of otolith shape to determine stock structure of *Engraulis encrasicolus* along the Tunisian coast. *Hydrobiologia*, 821, 73-82. https://doi.org/10.1007/s10750-017-3305-1

Kuhl, F.P. and Giardina, C.R., 1982. Elliptic Fourier features of a closed contour, *Computer Vision, Graphics, and Image Processing*, 18, 236-258.

Libungan, L.A. and Pálsson, S., 2015. ShapeR: An R Package to Study Otolith Shape Variation among Fish Populations. *PLOS ONE*, 10(**3**), e0121102. https://doi.org/10.1371/journal.pone.0121102.

Lombarte, A. and Cruz, A., 2007. Otolith size trends in marine fish communities from different depth strata. *Journal of Fish Biology*, 71, 53-76. https://doi.org/10.1111/j.1095-8649.2007.01465.x

Mapp, J., Hunter, E., Kooij, V.D., Songer, S. and Fisher, M., 2017. Otolith shape and size: The importance of age when determining indices for fish-stock separation. *Fisheries Research*, 190, 43-52. https://doi.org/10.1016/j.fishres.2017.01.017

Osman, A., Farrag, M., Mehanna, S. and Osman, Y., 2020. Use of otolithic morphometrics and ultrastructure for comparing between three goatfish species (family: Mullidae) from the northern Red Sea, Hurghada, Egypt. *Iranian Journal of Fisheries Sciences*. 19(**2**), 814-832. DOI: 10.22092/ijfs.2018.120044

Paul, K., Oeberst, R. and Hammer, C., 2013. Evaluation of otolith shape analysis as a tool for discriminating adults of Baltic cod stocks. *Journal of Applied Ichthyology*, 29(**4**), 743-750. https://doi.org/10.1111/jai.12145

Pavlov, D.A., 2019. Otolith Morphology of Amur Sleeper *Perccottus glenii* (Odontobutidae), *Journal of Ichthyology*, 59, 680-688. http://dx.doi.org/10.1134/S0032945219050114 R Project. https://www.r-project.org/about.html. Accessed 18 September 2021.

Sadighzadeh, Z., Otero-Ferrer, J.L., Lombarte, A., Fatemi, M.R. and Tuset, V.M., 2014. An approach to unraveling the coexistence of snappers (Lutjanidae) using otolith morphology. *Scientia Marina*, 78, 353-362. https://doi.org/10.3989/SCIMAR.03982.16C.

Sadighzadeh, Z., Valinassab, T., Vosiughi, G., Motallebi, A.A., Fatemi, M.R., Lombarte, A. and Tuset, V.M., 2014. Use of otolith shape for stock identification of John's snapper, *Lutjanus johnii* from the Persian Gulf and the Oman Sea. *Fisheries Research*, 155(**2014**) 59-63. https://doi.org/10.1015/j.fishres.2014.02-24.

Santos, R.D.S., Costa-de-Azevedoa, M.C., Albuquerque, C.D. and Araujo, F.G., 2017. Different sagittae otolith morphotypes for the white mouth croaker Micro pogonias fernier in the Southwestern Atlantic coast. *Fisheries Research*, 195, 222-229. https://doi.org/10.1016/j.fishres.2017.07.027

Sawusdee, A. and Rattanarat, J., 2021. Population dynamics of the Caroun croaker *Johnius carouna* (Cuvier, 1830) in coastal fishing ground in the middle gulf of Thailand. *Walailak Journal of Science and Technology*, 18, 1-8. https://doi.org/10.48048/wjst.2021.9611.

Schulz-Mirbach, T., Ladich, F., Plath, M., Metscher, B.D. and Heb, M., 2014. Are accessory hearing structures linked to inner ear morphology? Insights from 3D orientation patterns of ciliary bundles in three cichlid species. *Frontiers in Zoology*, 11, 1-25. https://doi.org/10.1186/1742-9994-11-25.

Stransky, C., 2005. Geographic variation of golden redfish (Sebastes marinus) and deep-sea redfish (*S. mentella*) in the North Atlantic based on otolith shape analysis. *ICES Journal of Marine Science*, 62(**8**), 1691-1698. https://doi.org/10.1016/j.icesjms.2005.05.012

Stransky, C., Baumann, H., Fevolden, S.E., Harbitz, A., Høie, H., Nedreaas, K.H., Salberg, A.B. and Skarstein, T., 2008. Separation of Norwegian coastal cod and Northeast Arctic cod by outer otolith shape analysis. *Fisheries Research*, 90, 26-35. https://doi.org/10.1016/J.FISHRES.2007.09.009.

Therneau, T.M. and Atkinson E.J., 2017. An Introduction to recursive partitioning using the rpart Routine. https://cran.r-project.org/web/packages/rpart, Accessed 180 September 2021.

Tran, D.T., 2015. Discussion on coastal zoning in Vietnam. *Institute of Marine Environment and Resources-VAST*, 10, 1-12. http://doi: 10.15625/1859-3097/15/1/4155

Tuset, V.M., Azzurro, E. and Lombarte, A., 2012. Identification of Lessepsian fish species using the sagittae otolith. *Scientia Marina*, 76, 289-299. http://doi:10.3989/SCIMAR.03420.18E.

Tuset, V.M., Farre, M., Otero-Ferrer, J.L., Vilar, A., Morales-Nin, B. and Lombarte, A., 2016. Testing otolith morphology for measuring marine fish biodiversity. *Marine and Freshwater Research*, 67, 1037-1048. http://dx.doi.org/10.1071/MF15052.

Volpedo, A.V. and Echeverra, D.D., 2003. Ecomorphological patterns of the sagitta in fish on the continental shelf off Argentine. *Fisheries Research*, 60, 551-560. https://doi.org/10.1016/S0165-7836(02)00170-4.

Vu, Q.T. and Kartavsev, Yu.Ph., 2020. Otolith shape analysis and its utilily for identification of two smelt species, *Hypomesus japonicus* and *H. nipponensis* (Osteichthyes, Osmeridae) from the northwestern Sea of Japan with inferences in stock discrimination of *H. japonicus*. *Russian Journal of Marine Biology*, 46, 431-440. https://doi.org/10.1134/S1063074020060115

Yedier, S., 2021. Otolith shape analysis and relationships between total length and otolith dimensions of European barracuda, *Sphyraena sphyraena* in the Mediterranean Sea. *Iranian Journal of Fisheries Sciences*. 20(**4**), 1080-1096.DOI: 10.22092/ijfs.2021.124429